Azeotropic Atom Transfer Radical Polymerization of Hydroxyethyl Methacrylate and (Dimethylamino)ethyl Methacrylate Statistical Copolymers and Block Copolymers with Polystyrene

Kyle B. Guice and Yueh-Lin Loo*

Department of Chemical Engineering, Center for Nano- and Molecular Science and Technology (CNM), University of Texas at Austin, 1 University Station, C0400, Austin, Texas 78712

Received December 13, 2005; Revised Manuscript Received January 29, 2006

ABSTRACT: Statistical copolymers of hydroxyethyl methacrylate (HEMA) and (dimethylamino)ethyl methacrylate (DMAEMA) were synthesized by atom transfer radical polymerization (ATRP) at the azeotrope in *N*,*N*-dimethylformamide (DMF) with controlled molecular weights and molecular weight distributions (generally <1.2). Since the polymerization takes place at the azeotrope, the polymer composition is fixed at the monomer feed composition (HEMA molar composition = 0.718), and there is little compositional drift with total monomer conversion. Poly(HEMA-*co*-DMAEMA) copolymers were also successfully synthesized from a polystyrene macroinitiator previously made by ATRP. Solution-cast thin films of polystyrene-*b*-poly(HEMA-*co*-DMAEMA) amphiphilic diblock copolymers exhibit ordered and periodic nanoscale structures with morphologies that depend on the relative volume fractions and casting solvent used.

Introduction

Free-radical polymerizations have been widely used in the synthesis of functional polymers because the active species—a free radical—is capable of propagating a variety of monomer and monomer functionalities. The recent development of "controlled" free-radical techniques, such as atom transfer radical polymerization (ATRP),[1] has led to improved control over molecular weight distributions of the resulting polymers. Additionally, since ATRP relies on radical capping and uncapping with a metal ligand complex, these polymerizations can be stopped and restarted at will during the course of the reactions. The combination of these attributes has made ATRP a useful polymerization scheme for synthesizing well-defined model polymers, and even functional block copolymers with drastically different chemical functionalities.[2] For example, hydroxyethyl methacrylate (HEMA) and (dimethylamino)ethyl methacrylate (DMAEMA) are two hydrophilic methacrylate monomers that cannot be easily polymerized by conventional anionic techniques. Yet, with ATRP, both poly(HEMA) and poly(DMAEMA) have been synthesized in controlled fashions.[3] In particular, HEMA can be successfully polymerized in both silyl-protected[4,5] and unprotected[6−11] forms; the resulting molecular weight distributions range from 1.1 to 1.5. DMAEMA homopolymerization by ATRP also results in polymers with narrow molecular weight distributions (<1.07).[10−14] Block copolymers of HEMA and DMAEMA with controlled molecular weight distributions have also been successfully demonstrated by ATRP.[11]

Poly(HEMA) is an important hydrophilic polymer, with current uses in contact lenses,[15] biocompatibilization,[16] and drug delivery.[17] Poly(DMAEMA) is a bioactive material that is responsive to changes in pH, as its tertiary amine functional group can be easily protonated below its pK_a of 7.5.[18] Micelles and amphiphilic networks of block copolymers containing HEMA[6] and/or DMAEMA[12,19,20] have therefore been investigated in controlled drug release applications.[21] In some cases, it is desirable to statistically copolymerize HEMA and DMAEMA to produce functional hybrid materials that combine the biocompatibility of HEMA with the pH responsiveness of DMAEMA.[21,22] Traditional copolymerization methods (generally photoinitiated free-radical polymerization in the presence of a cross-linker)[21] for creating HEMA−DMAEMA hydrogel networks, however, offer little control over comonomer distribution, cross-linking density, molecular weight, or molecular weight distribution. This limitation has in turn restricted the design and synthesis of model hydrogel systems.[20]

In this work, we report the synthesis and characterization of well-defined model hydrogels containing statistical copolymers of HEMA and DMAEMA. The statistical copolymer was synthesized at the compositional azeotrope[23] in *N*,*N*-dimethylformamide (DMF). The polymerization kinetics show a $t^{1/3}$ dependence, characteristic of ATRP reactions in a heterogeneous medium.[24] The resulting copolymers are narrow in molecular weight distributions (<1.2), indicating excellent control over the polymerization. Since the polymerizations were carried out at the azeotrope, little compositional drift along the polymer chain is observed, and the resulting polymer composition is that of the monomer feed composition. To demonstrate the versatility of this polymerization, poly(HEMA-*co*-DMAEMA) copolymers were also synthesized from a polystyrene macroinitiator made previously by ATRP. The resulting diblock copolymers also have narrow molecular weight distributions (≈1.15). When cast from neutral or near-neutral solvents, polystyrene-*b*-poly(HEMA-*co*-DMAEMA) diblock copolymers spontaneously microphase separate to produce ordered nanoscale structures depending on the volume fractions as well as the casting solvent.

Experimental Section

Materials. Styrene (Aldrich, 99%) and 2-(dimethylamino)ethyl methacrylate (DMAEMA, Acros, 98%) were passed through a column of activated basic alumina and stored over molecular sieves prior to use. 2-Hydroxyethyl methacrylate (HEMA, Acros, 98%) was purified by vacuum distillation (40 mTorr, 65 °C) to remove ethylene glycol dimethacrylate[6] prior to use. *N*,*N*-Dimethylforma-

* Corresponding author. E-mail: lloo@che.utexas.edu.

10.1021/ma052667h CCC: $33.50
Published on Web 02/24/2006

mide (DMF, Fisher Scientific) was dried over molecular sieves. 1-Bromoethylbenzene (Alfa Aesar, 97%), CuBr (Aldrich, 98%), CuCl (Aldrich, 98%), $CuBr_2$ (Aldrich, 98%), ethyl α-bromoisobutyrate (EB*i*B, Aldrich, 98%), *N*,*N*,*N*′,*N*″,*N*″-pentamethyldiethylenetriamine (PMDETA, Aldrich, 99%), and 1,2,4-trimethoxybenzene (Acros, 97%) were used as received.

Synthesis of Poly(HEMA-*co*-DMAEMA) Statistical Copolymer. HEMA (6.80 g, 51.2 mmol), DMAEMA (3.20 g, 20.0 mmol), CuCl (22.5 mg, 0.225 mmol), $CuBr_2$ (2.65 mg, 0.012 mmol), PMDETA (41.5 μL, 0.237 mmol), 6 mL of 1,2,4-trimethoxybenzene (gas chromatography standard), and 50 mL of DMF were added to a 100 mL flask equipped with a magnetic stir bar. The molar composition of the HEMA monomer, relative to the total monomer feed composition, was 0.718. This monomer feed composition was chosen because it represents the azeotropic composition[23] when copolymerization takes place in DMF; any other feed compositions would have resulted in compositional drifts along the final polymer (see Results and Discussion section for more details).[25] The flask was sealed with a septum, placed in an oil bath preheated to 45 °C, and purged with N_2 for 30 min. The reaction was then initiated by the addition of EB*i*B (35.9 μL, 0.237 mmol). Positive N_2 pressure was maintained throughout the polymerization. Aliquots were drawn at successive time points for a maximum time of 24 h for gas chromatography (GC) analysis. GC samples were diluted with acetone and injected without further purification. To terminate the polymerization, the remainder of each aliquot was cooled to 0 °C and then exposed to air. The polymerization medium was subsequently diluted with tetrahydrofuran (THF) and passed through neutral alumina to remove copper salts. The solution was then dialyzed against THF (10 mL of solution/100 mL of THF) for 24 h to remove DMF. Upon further concentration, the solution was precipitated into hexanes. The filtered polymer was dried in vacuo at room temperature for 24 h.

Synthesis of Bromine-Terminated Polystyrene Macroinitiator by ATRP. Styrene (13.6 g, 127 mmol), CuBr (186 mg, 1.30 mmol), $CuBr_2$ (14.2 mg, 0.060 mmol), PMDETA (233 μL, 1.33 mmol), and 30 mL of anisole were added to a 100 mL flask equipped with a magnetic stirrer bar. The flask was sealed with a septum, placed in an oil bath preheated to 110 °C, and purged with N_2 for 30 min. The reaction was then initiated by the addition of 1-bromoethylbenzene (235 μL, 1.30 mmol) and was carried out for 3 h and 50 min. The reaction flask was removed from the oil bath and cooled to 0 °C, and the solution was exposed to air; this procedure terminated the polymerization. The solution was then diluted with THF and passed through neutral alumina to remove copper salts. Finally, the solution was concentrated and precipitated into methanol. The polymer was collected by filtration and was dried in vacuo for 24 h to yield a polystyrene macroinitiator with an absolute number-average molecular weight of 6500 g/mol and a molecular weight distribution of 1.02, as determined by gel permeation chromatography (GPC) with THF as eluent.

Synthesis of Polystyrene-*b*-poly(HEMA-*co*-DMAEMA) Diblock Copolymers. HEMA, DMAEMA, CuCl, $CuBr_2$, PMDETA, and 1,2,4-trimethoxybenzene were added to a 100 mL flask equipped with a magnetic stir bar in the same molar ratios as those for the statistical copolymerization of HEMA and DMAEMA described above. To study the effects of compositional drift, we also carried out a separate polymerization away from the azeotrope, at a HEMA molar monomer composition of 0.25. In this particular case, 2.40 g of HEMA (17.8 mmol) and 8.60 g of DMAEMA (53.3 mmol) were used instead of the previously noted quantities. 40 mL of DMF was also added to the reaction flask. The flask was sealed with a septum, placed in an oil bath preheated to 45 °C, and purged with N_2 for 30 min. Separately, the polystyrene macroinitiator (1.54 g, 0.237 mmol) in 10 mL of DMF was preheated at 45 °C and purged with N_2 for 30 min. The reaction was initiated by adding the warm macroinitiator solution to the reaction flask. Aliquots were taken throughout the reaction, and GC analysis and subsequent polymer cleanup proceeded as described above for poly(HEMA-*co*-DMAEMA) copolymers. Polystyrene-*b*-poly(HEMA-*co*-DMAEMA) polymer samples will be referred to as S/HD *x*/*y*, with *x* and *y* being the absolute number-average molecular weights of the polystyrene and poly(HEMA-*co*-DMAEMA) blocks, reported in kg/mol, respectively.

Characterization. GC was carried out on an Agilent Technologies 6850 Series II Network GC system equipped with a poly(dimethylsiloxane) capillary column (12 m × 200 μm × 0.25 μm) with H_2 as eluent at a flow rate of 1.5 mL/min and with a temperature ramp rate of 10 °C/min and a flame ionization detector operating at 300 °C with a H_2 flow rate of 40 mL/min. 1,2,4-Trimethoxybenzene (1/1 v/v to HEMA) was added to the polymerization medium as an internal GC standard. GC samples were diluted with acetone prior to characterization. ^{1}H NMR spectroscopy was performed in deuterated DMF on a Varian Unity+ 300 MHz NMR spectrometer. An Optilab DSP interferometric refractometer (Wyatt Technology Corp.) was used to measure the d*n*/d*c* of poly(HEMA-*co*-DMAEMA) in DMF at varying concentrations. Gel permeation chromatography was performed using a GPC system equipped with a Waters 515 HPLC solvent pump, two PLgel mixed-C columns (5 μm bead size, MW range 200−2 000 000 g/mol, Polymer Laboratories Inc.) connected in series with the same interferometric refractometer used for d*n*/d*c* measurements and a multiangle laser light scattering (MALLS) detector (λ = 690 nm, DAWN-EOS, Wyatt Technology Corp.). DMF with 0.05 M LiBr[26] (Aldrich) was used as the mobile phase at a flow rate of 1.0 mL/min at 60 °C. The absolute molecular weights of polystyrene macroinitiators and poly(HEMA-*co*-DMAEMA) statistical copolymers were obtained from GPC data given known[27] and calculated d*n*/d*c* values, respectively. The absolute molecular weights of polystyrene-*b*-poly(HEMA-*co*-DMAEMA) block copolymers were determined given the absolute molecular weight of the appropriate polystyrene macroinitiator and ^{1}H NMR compositional analysis (see Results and Discussion section for more details). Small-angle X-ray scattering (SAXS) was performed in a long-range sample chamber, and scattered photons were collected on a 2D multiwire gas-filled detector (Molecular Metrology, Inc.). X-rays were produced by a rotating copper anode X-ray generator (Bruker Nonius; λ = 1.5406 Å) operating at 3.0 kW. The scattering angle was calibrated with a silver behenate ($CH_3(CH_2)_{20}COOAg$) standard. SAXS profiles were acquired for 2 h.

Results and Discussion

Kinetics of Poly(HEMA-*co*-DMAEMA) Azeotropic Copolymerization. HEMA and DMAEMA were copolymerized in DMF by ATRP with EB*i*B. We chose a mixed halide system consisting of a bromine initiator (EB*i*B) and a CuCl catalyst. The use of mixed halide systems to better control ATRP polymerizations was first reported for the synthesis of poly(methyl methacrylate), PMMA.[28] In particular, EB*i*B has a higher rate of initiation relative to its chlorine counterpart (ethyl 2-chloroisobutyrate), while CuCl has slower propagation compared to CuBr.[28,29] There is therefore consensus that the use of such mixed halide initiator−catalyst systems can result in faster initiation but better controlled propagation,[28] which in turn can improve control over molecular weights and can generally lead to narrower molecular weight distributions. It follows that such mixed halide systems are especially effective for the polymerization of monomers with high propagation constants, such as HEMA.[30] We also added $CuBr_2$ at the onset of polymerization to help maintain a decent rate of radical deactivation and to effectively suppress the rate of radical termination.[31]

The kinetics of poly(HEMA-*co*-DMAEMA) copolymerization are shown in Figure 1 (■). The polymerization kinetics do not obey classical first-order ATRP kinetics,[32] nor do they proceed with a $t^{2/3}$ dependence, as suggested by the persistent radical effect theory.[33,34] Rather, our poly(HEMA-*co*-DMAEMA) polymerization kinetics data appear to be described by a $t^{1/3}$

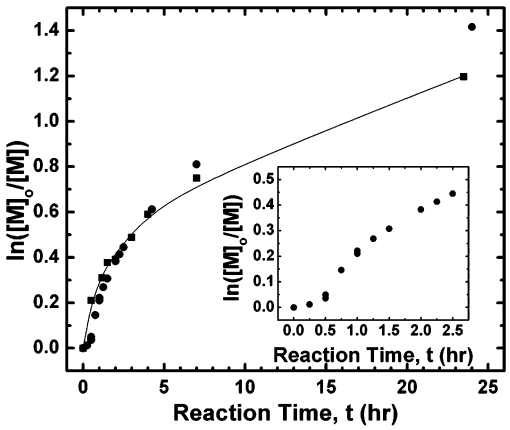

Figure 1. Kinetic plot for the azeotropic atom transfer radical polymerization of poly(HEMA-*co*-DMAEMA) at 45 °C in *N*,*N*-dimethylformamide with ethyl α-bromoisobutyrate as the initiator (■) and from a polystyrene macroinitiator of 6.5 kg/mol (●). Inset: polymerization kinetics from the polystyrene macroinitiator at early times (<3 h).

dependence, as proposed by Snijder et al. (eq 1).[24]

$$\ln\frac{[M]_0}{[M]} = \frac{k_p[Cu^{II}]_c}{2k_{tD}K_{eq}}\left\{\left(6k_{tD}\left(\frac{K_{eq}}{[Cu^{II}]_c}\right)^2 t + [RX]_0\right)^{1/3} - [RX]_0^{-1}\right\} \quad (1)$$

In eq 1, $[M]_0$ is the initial monomer concentration, [M] is the monomer concentration at any given time t, k_p is the propagation rate constant, k_{tD} is the rate constant of termination by disproportionation, K_{eq} is the equilibrium constant for the capping and uncapping reactions at the radical chain end, $[RX]_0$ is the initial initiator concentration, and $[Cu^{II}]_c$ is the Cu^{II} ceiling concentration, which remains constant throughout the course of the polymerization. The classical first-order ATRP kinetics[32] assume a constant radical concentration and is only valid when the overall radical concentration is sufficiently low. Consequently, such kinetics have been observed in polymerizations where the free radical is largely dormant (capped by metal−ligand complex) or when the Cu^I catalyst concentration is sufficiently low and the Cu^{II} concentration is sufficiently high.[32] Fischer's persistent radical effect theory,[33] which predicts $t^{2/3}$ dependence, is valid when little or no Cu^{II} is added to the polymerization medium. In both cases, the reaction medium is homogeneous; i.e., the metal−ligand complex is well solubilized. The Snijder model was developed to describe heterogeneous ATRP polymerizations. In particular, this model invokes the notion of a Cu^{II} deactivator ceiling concentration, $[Cu^{II}]_c$, above which excess Cu^{II} will precipitate from the polymerization medium. Heterogeneous polymerizations[24] of methyl methacrylate in the presence of $Cu^IBr/Cu^{II}Br_2$/PMDETA have validated this model.

Visually, the conditions we used to copolymerize HEMA and DMAEMA result in a heterogeneous reaction medium; a trace amount of yellow-green Cu^{II} precipitant was observed at the bottom of the reaction flask shortly after initiation. As such, we are not surprised that our kinetics data are described by the model proposed by Snijder and co-workers[24] and not by the classical first-order kinetics or the persistent radical effect theory. To fit our data, we simplified eq 1 above into an expression with two lumped kinetic parameters, A and B (eq 2).

$$\ln\frac{[M]_0}{[M]} = A\{(Bt + [RX]_0)^{1/3} - [RX]_0^{-1}\} \quad (2)$$

Subjecting our data to a best fit yields $A = 8.41 \times 10^{-4}$ mol L^{-1} and $B = 5.59 \times 10^4$ L^3 mol^{-3} s^{-1} (correlation coefficient = 0.9957).

We also synthesized block copolymers of polystyrene-*b*-poly(HEMA-*co*-DMAEMA). These block copolymers were synthesized from a polystyrene macroinitiator that was previously made by ATRP (M_n = 6500 g/mol; M_w/M_n = 1.02). The polymerization kinetics of poly(HEMA-*co*-DMAEMA) from a 6500 g/mol polystyrene macroinitiator are also shown in Figure 1 (●). The kinetics data are quantitatively similar to that of poly(HEMA-*co*-DMAEMA) copolymerization with EB*i*B (■), and the polymerization proceeds with $t^{1/3}$ kinetics. There is, however, a subtle difference between the two polymerizations: there is an induction period of ~30 min during the onset of copolymerization from the polystyrene macroinitiator. The early times data (<3 h) are provided in the inset of Figure 1. Specifically, the reaction appears to start off slowly but subsequently proceeds at the rate with which poly(HEMA-*co*-DMAEMA) is polymerized when the reaction is initiated with EB*i*B. We carried out similar polymerizations with a polystyrene macroinitiator of a different molecular weight (M_n = 3200 g/mol; M_w/M_n = 1.02). The kinetics data also showed an induction period during the early stages of polymerization. Consistent with the kinetics data, we observed a slower color change (from dull teal to bright blue; indication of "controlled" polymerization) after the polystyrene macroinitiator was added to the reaction medium. This delay in initiation, however, was not observed when the copolymerization was initiated with EB*i*B. Rather, the color change was almost instantaneous when we initiated the copolymerization with EB*i*B. We presently do not understand the origin of this delayed initiation. We speculate, however, that this slow initiation is associated with the solubility of polystyrene in DMF. Polystyrene has a solubility parameter[25] of $\delta_{PS} = 9.0$ $(cal/cm^3)^{1/2}$ while DMF has a solubility parameter[27] of $\delta_{DMF} = 12.1$ $(cal/cm^3)^{1/2}$. One can therefore imagine that the active chain ends are buried in the rather collapsed coils of polystyrene in DMF. The delayed initiation is thus likely to be related to the time needed for the first monomers to access the active chain ends. To definitively explain the induction period we observe, experiments varying the solubility parameter difference between the macroinitiator and the solvent will have to be carried out. Changing the solvent quality, however, is complicated because it will necessarily impact the reactivity ratios of HEMA and DMAEMA, which will in turn affect the compositional uniformity in the poly(HEMA-*co*-DMAEMA) that is formed subsequently. We have therefore chosen to carry out HEMA and DMAEMA copolymerizations in DMF using other macroinitiators, e.g., poly(*tert*-butyl acrylate),[35] to verify our hypothesis. These experiments are currently underway. We note that other groups have also reported slow initiation from macroinitiators,[19,36] although explanations for such phenomenon were not provided. We stress that this slow initiation from the polystyrene macroinitiator does not impact our ability to control the composition or the molecular weight distribution of the resulting copolymers.

Figure 2 contains an ^1H NMR spectrum of S/HD 6.5/27. The proton contributions are labeled for clarity: peaks **a** (δ = 7.14 ppm, 6.69 ppm; 5H) are characteristic of the aromatic hydrogens (of styrene repeat units), peak **b** (δ = 4.04 ppm; 2H) is characteristic of the α hydrogens off of the ester group in both HEMA and DMAEMA repeat units, peak **c** (δ = 3.74 ppm; 2H) is characteristic of the ethyl hydrogens in HEMA, peak **d** (δ = 2.57 ppm; 2H) is characteristic of ethyl hydrogens in DMAEMA, peak **e** (δ = 2.25 ppm; 6H) is characteristic of

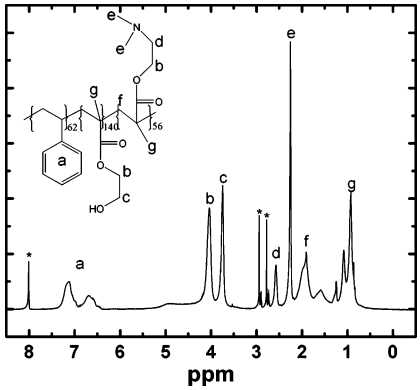

Figure 2. ^{1}H NMR spectrum of polystyrene-*b*-poly(HEMA-*co*-DMAEMA) ($M_{n,polystyrene}$ = 6.5 kg/mol, $M_{n,total}$ = 33.5 kg/mol) in deuterated *N*,*N*-dimethylformamide. * indicates solvent peaks.

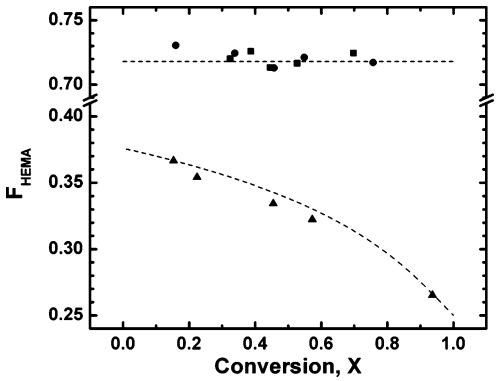

Figure 3. Hydroxyethyl methacrylate (HEMA) molar polymer compositions during three separate atom transfer radical polymerizations of poly(HEMA-*co*-DMAEMA): at the azeotrope (f_{HEMA} = 0.718) with ethyl α-bromoisobutyrate as the initiator (■), at the azeotrope from a polystyrene macroinitiator of 6.5 kg/mol (●), and outside the azeotrope (f_{HEMA} = 0.25) from the same polystyrene macroinitiator (▲). Dashed curves indicate the time-averaged polymer composition; we integrated the instantaneous polymer compositions predicted by the Skiest equation to obtain these curves.

hydrogens off of the tertiary amine in DMAEMA, and peaks **f**, **g** (δ = 0.80−2.10 ppm) are backbone hydrogens. The molar composition of polystyrene in the diblock copolymer was determined to be 0.240 based on the relative areas of peaks **a** (styrene) and **b** (methacrylate). To determine the HEMA composition (F_{HEMA}) within the methacrylate block, we quantified the relative areas of peaks **b** (both HEMA and DMAEMA) and **e** (DMAEMA). The HEMA molar composition within the methacrylate block is 0.713, and is consistent with the azeotropic molar feed composition for the copolymerization.

Azeotropic Considerations. We characterized all the aliquots collected during the polymerization of poly(HEMA-*co*-DMAEMA) with EB*i*B (■) and that from the polystyrene macroinitiator (●) by ^{1}H NMR (representative spectrum in Figure 2); the HEMA molar compositions (F_{HEMA}) within the methacrylate blocks are shown in Figure 3. Given the published reactivity ratios of the monomers (r_{HEMA} = 0.75 and r_{DMAEMA} = 0.36),[23] the Skiest equation[37] predicts an azeotrope at HEMA molar feed composition of f_{HEMA} = 0.718. Since both the copolymerizations were carried out at the azeotrope, compositional uniformity along the polymer chains is expected. That F_{HEMA} is constant at 0.72 ± 0.10 at any given point during both the reactions verifies that there is little to no compositional drift along the methacrylate block of the polymers, whether the polymerization is initiated with EB*i*B or by a polystyrene macroinitiator.

Accordingly, polymerizations at feed compositions other than the azeotropic composition are expected to produce significant compositional drifts along the polymer chain. To illustrate this, we carried out a poly(HEMA-*co*-DMAEMA) copolymerization from the same polystyrene macroinitiator at f_{HEMA} = 0.25. Aliquots were taken at several points during the reaction, and we determined the time-averaged polymer compositions for each aliquot by ^{1}H NMR. The time-averaged HEMA molar fractions within the methacrylate block are plotted against the total monomer conversion in Figure 3 (▲). At early times or low conversions, the methacrylate block is enhanced in HEMA ($F_{HEMA} > f_{HEMA}$) given that $r_{HEMA} > r_{DMAEMA}$. As the reaction progresses, HEMA monomers are depleted faster than DMAEMA monomers so the tail of the methacrylate block is enhanced in DMAEMA (relative to feed composition). For this particular feed composition, the Skiest equation[23] predicts an initial polymer HEMA molar composition of 0.375. This prediction is consistent with our initial data point. In the limit of complete monomer conversion, F_{HEMA} should equal f_{HEMA} at 0.25. We also observe this to be true in our experiments. Since the Skiest equation only predicts the instantaneous polymer composition,[25] we integrated the instantaneous polymer composition to estimate the time-averaged polymer composition as a function of monomer conversion. The dashed lines in Figure 3 represent the time-averaged polymer composition, predicted by the Skiest equation with reactivities of r_{HEMA} = 0.75 and r_{DMAEMA} = 0.36, at the azeotrope, and at f_{HEMA} = 0.25. Our experimental results agree well with the values predicted by the Skiest equation and implicate the importance of polymerization at the azeotrope to eliminate compositional heterogeneity along the polymer chain. Copolymerization outside the azeotrope, such as that at f_{HEMA} = 0.25, results in a gradient copolymer, rather than a statistical copolymer, that is enriched in HEMA at the onset and in DMAEMA in the tail.

Molecular Weight Distribution. Polymers collected during the azeotropic polymerizations with EB*i*B, and from the polystyrene macroinitiator, were analyzed by GPC with DMF (+ 0.05 M LiBr) as the eluent. LiBr was added to suppress polymer−solvent and polymer−substrate interactions that are typically observed in polymers with ionic functional groups.[38,39] GPC traces for each of the aliquot collected during the polymerizations are shown in Figure 4. Parts a and b of Figure 4 contain the GPC time evolution of aliquots collected during the copolymerization with EB*i*B and from the polystyrene macroinitiator, respectively. Characteristic of ATRP, the GPC traces are narrow, symmetric, and monomodal; the extracted molecular weight distributions are each less than 1.2, with the exception of the last aliquot collected during the diblock copolymerization (explanation provided below). As the reactions progress, the peaks shift to smaller elution volumes, indicating a time-dependent increase in molecular weight during both polymerizations.

We determined the absolute number-average molecular weight of our polystyrene macroinitiator (M_n = 6500 g/mol; M_w/M_n = 1.02) using GPC with THF as the eluent. For comparison, we also analyzed the same polystyrene macroinitiator by GPC with DMF and 0.05 M LiBr as the eluent. In this case, the polystyrene macroinitiator elutes at a much higher elution volume (18.15 mL). In fact, the polystyrene macroinitiator peak overlaps the solvent peak in the GPC trace in Figure 4b despite real differences in molecular weights between the two. Though peculiar at first glance, this phenomenon has previously been reported by Dubin and co-workers where low molecular weight polystyrene samples (<4000 g/mol) elute at the same volume as polar small molecules when GPC is performed in DMF.[39] The presence of salt (0.1 M LiBr) shifts

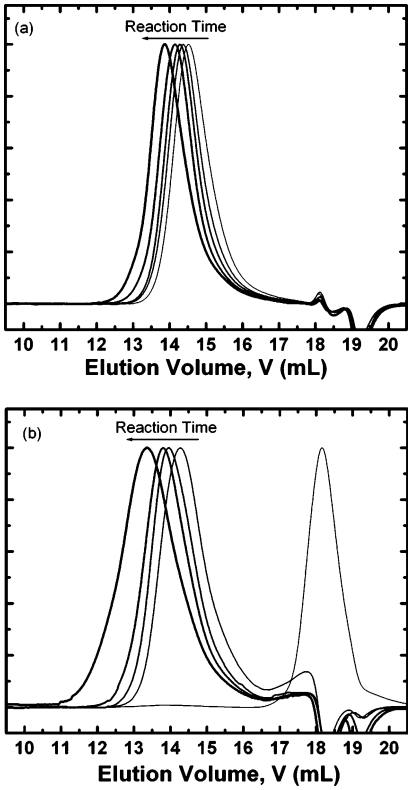

Figure 4. Gel permeation chromatography traces with *N*,*N*-dimethylformamide (+ 0.05 M LiBr) as the eluent at 1 mL/min, showing the time-dependent molecular weight evolution during the polymerization of (a) poly(HEMA-*co*-DMAEMA) and (b) polystyrene-*b*-poly(HEMA-*co*-DMAEMA).

the polymer peak to even higher elution volumes.[26] This "salting out" phenomenon observed with polystyrene is caused by a reduction in the solubility of the polymer in the eluent, which is manifested by a decrease in the effective hydrodynamic volume so a larger elution volume is measured.[39] As a reference, we also measured a polystyrene standard of a slightly higher absolute molecular weight (M_n = 7800 g/mol, M_w/M_n = 1.05) under the same conditions. This polystyrene standard also elutes near the solvent peak, at 17.95 mL.

The methacrylate block number-average molecular weights for both polymerizations (■, ●) are compiled in Figure 5. The absolute number-average molecular weights for the polymers collected during the copolymerization with EB*i*B (■) were extracted from GPC data using a d*n*/d*c* of 0.1009 (±0.0067; measured independently with an interferometric refractometer from five concentrations of poly(HEMA-*co*-DMAEMA) in DMF with 0.05 M LiBr). The absolute number-average molecular weights of the methacrylate block in polystyrene-*b*-poly(HEMA-*co*-DMAEMA) diblock copolymers (●) were obtained by ^{1}H NMR, given an absolute M_n for the polystyrene macroinitiator. In both polymerizations, the molecular weight increases linearly with total monomer conversion. Additionally, the increase in molecular weights in both polymerizations appear to be well described by a single fit (dashed line is fit to both sets of molecular weight data). Both features are characteristic of ATRP polymerization and indicate controlled reactions. We note, however, that the molecular weight at any given conversion is higher than the theoretical molecular weight predicted by the initial monomer and initiator concentrations (solid line). We also carried out polymerizations at a different monomer to initiator molar ratio ($[M]_0:[I]_0$ = 150:1 instead of 300:1). The polymer molecular weights in this case are also higher than the

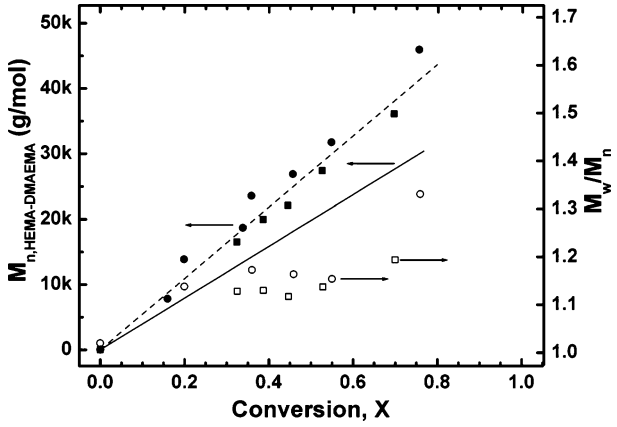

Figure 5. Molecular weight plot for the azeotropic atom transfer radical polymerization of poly(HEMA-*co*-DMAEMA) with ethyl α-bromoisobutyrate as the initiator (■, □) and from a polystyrene macroinitiator (●, ○). The absolute number-average molecular weight of the methacrylate block (M_n; ■, ●) is plotted on the left axis, and the overall molecular weight distribution (M_w/M_n; □, ○) is plotted on the right axis. Dashed line represents a single fit through both sets of molecular weight data while solid line represents the theoretical molecular weight given the initial monomer-to-initiator ratio.

theoretical molecular weights, but they are well described by the same dashed line fit when we scale the molecular weights by the monomer-to-initiator ratio. Higher than expected molecular weights during ATRP polymerizations are not uncommon and have been observed by many others.[6,11] While we do not yet have a clear explanation for this observation, we suspect inefficiency during initiation to be responsible. This initiation inefficiency appears to be constant and independent of the types of initiator used (whether EB*i*B or polystyrene macroinitiator) and monomer-to-initiator ratios (whether $[M]_0:[I]_0$ = 150:1 or 300:1). So well-defined poly(HEMA-*co*-DMAEMA) copolymers and block copolymers of desired molecular weights can still be tailor-made, given the information in Figure 5.

The molecular weight distributions (□, ○) for each of the aliquot collected during both polymerizations remain narrow (<1.2 for copolymers from EB*i*B and ≈1.15 for block copolymers from the polystyrene macroinitiator), indicating that the polymerizations are under control throughout. The final block copolymer sample (S/HD 6.5/46), however, exhibits a higher molecular weight distribution (M_w/M_n = 1.33) compared to the other aliquots. Since this particular aliquot was collected after >24 h reaction, we suspect a gradual loss in the metal−ligand complex activity to be responsible for the slight increase in its molecular weight distribution. We note that we typically limit the total monomer conversion to <60% when we make polystyrene-*b*-poly(HEMA-*co*-DMAEMA) diblock copolymers for structural characterization. These block copolymers all exhibit molecular weight distributions ≈1.15. For example, the two block copolymers that are used in the present SAXS study have molecular weight distributions of 1.14 and 1.16.

Small-Angle X-ray Scattering (SAXS). We assessed the solid-state morphologies of polystyrene-*b*-poly(HEMA-*co*-DMAEMA) thin films that were cast from solutions of both DMF and THF (0.2 mg/mL). The block copolymer solution was poured into Teflon casting dishes, and the solvent was allowed to evaporate slowly under a partially covered Petri dish. Because of its high volatility, THF generally evaporated over the course of 24 h while DMF (with a higher boiling temperature of 153 °C)[40] evaporated over ≈6 days. The films were then peeled from the casting dish and dried in the vacuum oven at 40 °C for an additional 24 h. The average film thickness is 0.40 ± 0.05 mm. We calculated the volume fractions of the block copolymers

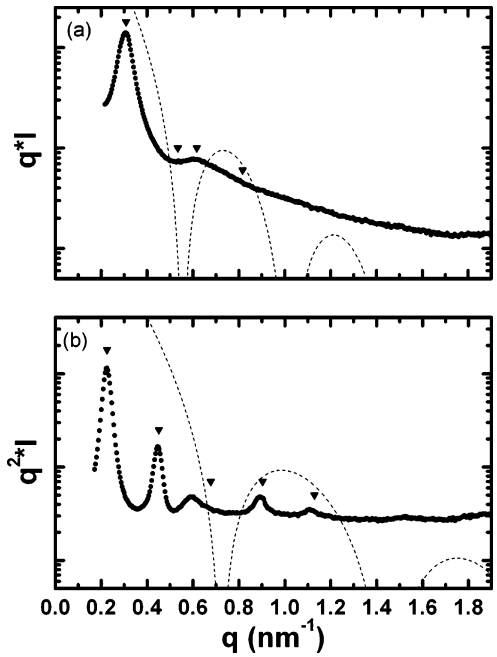

Figure 6. Small-angle X-ray scattering profiles of polystyrene-*b*-poly(HEMA-*co*-DMAEMA) ($M_{n,polystyrene}$ = 6.5 kg/mol, $M_{n,total}$ = 22.5 kg/mol) cast from (a) *N*,*N*-dimethylformamide and (b) tetrahydrofuran.

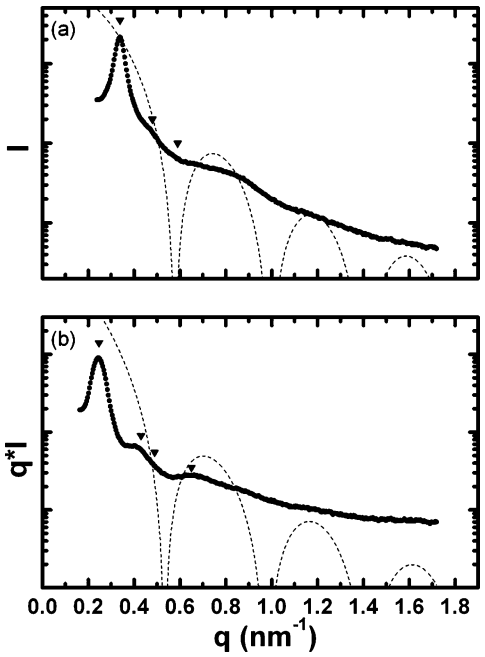

Figure 7. Small-angle X-ray scattering profiles of polystyrene-*b*-poly(HEMA-*co*-DMAEMA) ($M_{n,polystyrene}$ = 6.5 kg/mol, $M_{n,total}$ = 33.5 kg/mol) cast from (a) *N*,*N*-dimethylformamide and (b) tetrahydrofuran.

using a published polystyrene homopolymer density[27] of 1.05 g/cm^3. Separately, we determined the density of poly(HEMA-*co*-DMAEMA) according to ASTM D153-84,[41] method C, to be 1.20 ± 0.01 g/cm^3 using a pycnometer with cyclohexane as the nonsolvent.

SAXS traces for S/HD 6.5/16 (υ_s = 0.312) cast from DMF and from THF are shown in the top and bottom portions of Figure 6, respectively. In the top SAXS trace, we observe a narrow and intense primary peak, followed by a higher-order reflection at approximately q = 0.6 nm^{-1}. Given the volume fraction of S/HD 6.5/16, we expect this sample to adopt a hexagonally-packed cylindrical morphology (CYL with polystyrene cylinders). Accordingly, we placed markers (▼) at q/q^* ratios of 1, $\sqrt{3}$, $\sqrt{4}$, and $\sqrt{7}$ for comparison. The higher-order peak corresponds to $q/q^* = \sqrt{4}$ of the CYL morphology. For completeness, we also plotted the form factor curve[42] (dashed line). Since the first form factor minimum coincides with $q/q^* = \sqrt{3}$, the structure factor peak is suppressed in the overall SAXS trace. Given the primary peak location (q^* = 0.3086 nm^{-1}) and the volume fraction, we calculate the spacing between the (10) planes to be 20.36 nm and an average cylindrical radius of 6.89 nm. The SAXS trace from the THF-cast film of S/HD 6.5/16 (bottom of Figure 6) also shows a narrow and intense primary peak, but with characteristic peaks at q/q^* = 2, 4, and 5, indicating an alternating lamellar (LAM) morphology instead of the CYL morphology. The form factor curve corresponding to LAM[42] with υ_s = 0.312 is provided (dashed line). The third-order reflection is suppressed in this case due to its coincidence with a form factor minimum. On the basis of the primary peak position (q^* = 0.2258 nm^{-1}), we estimate the characteristic spacing to be 27.83 nm. Additionally, we note a broader and less intense peak at $q/q^* = \sqrt{7}$. While the $\sqrt{7}$ reflection should not be observed in LAM, it is characteristic of CYL. We therefore suspect a coexistence of LAM and CYL in this cast film. Yet, the peak at $q/q^* = \sqrt{3}$ (q = 0.3911 nm^{-1}), also characteristic of CYL, is absent. Given how narrow the primary peak is (fwhm = 0.038 nm^{-1}), the lamellae and cylinders, if present, must share the same characteristic spacing or the same q^*. That LAM and CYL phases share the same characteristic spacing due to epitaxial phase transformation has previously been reported.[43] We calculated the form factor curve based on the same q^* assuming a CYL morphology. The first minimum in the cylinder form factor curve occurs at q = 0.4066 nm^{-1}, which is likely the reason why the $\sqrt{3}$ reflection is not observed. Since this specimen has not been thermally annealed above the glass transition temperatures of either of the blocks, the solid-state morphology is a reflection of the casting conditions. We are therefore not surprised to see coexistence of two neighboring phases in our specimen. We are also not surprised to see differences in morphologies from the two different castings. In fact, the difference in morphologies (CYL vs LAM) due to changes in the solvent quality (DMF vs THF) is entirely consistent with solubility parameter arguments. Published solubility parameters, δ_{DMF}[27] = 12.1 (cal/cm^3)$^{1/2}$, δ_{THF}[27] = 9.1 (cal/cm^3)$^{1/2}$, δ_{PS}[25] = 9.0 (cal/cm^3)$^{1/2}$, and δ_{PHEMA}[44] = 13.2 (cal/cm^3)$^{1/2}$, indicate that THF is a better solvent for polystyrene than DMF and that DMF is a better solvent for poly(HEMA) compared with THF. (An exact comparison with poly(HEMA-*co*-DMAEMA) is difficult because the solubility parameter of the copolymer is not available.) As such, the volume occupied by the polystyrene block must be greater when S/HD 6.5/16 is cast from THF compared to DMF.

SAXS traces for S/HD 6.5/27 (υ_s = 0.216) are shown in Figure 7. The top trace is acquired on a DMF-cast film, while the bottom trace is acquired on a THF-cast film. The SAXS trace acquired on the DMF-cast film shows a narrow and intense peak followed by a shoulder at $q/q^* = \sqrt{2}$, indicating a body-centered cubic spherical (SPH) morphology. The sphere form factor[42] curve is also plotted (dashed line). The higher-order structure factor peak at $q/q^* = \sqrt{3}$ is absent because it coincides with a form factor minimum. We also observe a broad bump in the overall SAXS trace between 0.65 and 0.9 nm^{-1} that corresponds to a maximum in the sphere form factor curve. Given the primary peak position (q^* = 0.3381 nm^{-1}) and the volume fraction, we estimate the spacing between (100) planes to be 18.59 nm and an average spherical radius of 7.77 nm. The SAXS trace acquired on the THF-cast film, on the other hand, shows a primary peak and a higher-order peak at q/q^* =

$\sqrt{3}$ that is characteristic of the CYL morphology. The cylinder form factor curve is plotted (dashed line); the minima and maxima appear to correspond well with the overall SAXS trace. The primary peak position is $q^* = 0.2468$ nm^{-1}, indicating a characteristic spacing of 25.46 nm, with an average cylindrical radius of 7.18 nm. Consistent with S/HD 6.5/16, we observe a shift in the solid-state morphology of S/HD 6.5/27 with different solvents. A similar transition has also been observed by transmission electron microscopy for polystyrene-*b*-poly(HEMA) block copolymers.[45] In this work, the authors suggest that DMF preferentially solvates the HEMA block, producing structures outside the predicted morphology. We note, however, that DMF castings of both block copolymers produce morphologies that are closer to the expected equilibrium structure predicted by the mean-field theory[46] given the actual volume fractions. To ascertain the equilibrium morphologies for these block copolymers, high-temperature annealing above the glass transition temperatures of both blocks is undoubtedly necessary. Our initial attempts to reach thermal equilibrium, however, were limited by transesterification side reactions that served to cross-link the poly(HEMA-*co*-DMAEMA) block.[47,48]

Conclusions

We successfully produced model hydrogels consisting of well-defined poly(HEMA-*co*-DMAEMA) statistical copolymers. The copolymerizations were carried out at the azeotrope to ensure compositional uniformity along the polymer chain. The polymerization medium is heterogeneous; reaction kinetics exhibit a $t^{1/3}$ dependence, rather than being first-order. Characteristic of controlled free radical polymerizations, the number-average molecular weight increases linearly with conversion, and the molecular weight distribution is narrow throughout the reaction. Well-defined polystyrene-*b*-poly(HEMA-*co*-DMAEMA) diblock copolymers can be synthesized using a polystyrene macroinitiator in place of an ATRP initiator; these diblocks microphase separate on solution casting to form ordered and periodic nanostructures.

Acknowledgment. This work is funded by the National Science Foundation (NSF CAREER DMR-0348339) and a Camille and Henry Dreyfus New Faculty Award. Support from the Keck Foundation, the Welch Foundation, and Texas Materials Institute is also gratefully acknowledged. K.B.G. acknowledges the NSF for a graduate fellowship. We thank Dr. Chris Bielawski and Dan Coady for assistance with GC measurements and Tracy Bucholz for help with SAXS measurements.

References and Notes

(1) Coessens, V.; Pintauer, T.; Matyjaszewski, K. *Prog. Polym. Sci.* **2001**, *26*, 337−377.
(2) Matyjaszewski, K.; Xia, J. In *Handbook of Radical Polymerization*; Matyjaszewski, K., Davis, T., Eds.; Wiley-Interscience: New York, 2002.
(3) Tsarevsky, N. V.; Pintauer, T.; Matyjaszewski, K. *Macromolecules* **2004**, *37*, 9768−9778.
(4) Beers, K. L.; Gaynor, S. G.; Matyjaszewski, K.; Sheiko, S. S.; Moller, M. *Macromolecules* **1998**, *31*, 9413−9415.
(5) Li, Z.; Day, M.; Ding, J.; Faid, K. *Macromolecules* **2005**, *38*, 2620−2625.
(6) Weaver, J. V. M.; Bannister, I.; Robinson, K. L.; Bories-Azeau, X.; Armes, S. P. *Macromolecules* **2004**, *37*, 2395−2403.
(7) Robinson, K. L.; Khan, M. A.; de Paz Báñez, M. V.; Wang, X. S.; Armes, S. P. *Macromolecules* **2001**, *34*, 3155−3158.
(8) Beers, K. L.; Boo, S.; Gaynor, S. G.; Matyjaszewski, K. *Macromolecules* **1999**, *32*, 5772−5776.
(9) Simal, F.; Demonceau, A.; Noels, A. F. *Angew. Chem., Int. Ed.* **1999**, *38*, 538−540.
(10) Monge, S.; Darcos, V.; Haddleton, D. M. *J. Polym. Sci., Part A: Polym. Chem.* **2004**, *42*, 6299−6308.
(11) Jin., X.; Shen, Y.; Zhu, S. *Macromol. Mater. Eng.* **2003**, *288*, 925−935.
(12) Lee, S. B.; Russell, A. J.; Matyjaszewski, K. *Biomacromolecules* **2003**, *4*, 1386−1393.
(13) Mao, B.; Gan, Y.-Y.; Li, X.; Ravi, P.; Tam, K.-C. *J. Polym. Sci., Part A: Polym. Chem.* **2004**, *42*, 5161−5169.
(14) Zhang, X.; Xia, J.; Matyjaszewski, K. *Macromolecules* **1998**, *31*, 5167−5169.
(15) Wilcox, M. D. P.; Harmis, N.; Cowell, B. A.; Williams, T.; Holden, B. A. *Biomaterials* **2001**, *22*, 3235−3247.
(16) Jeyanthi, R.; Rao, K. P. *Biomaterials* **1990**, *11*, 238−243.
(17) Abraham, S.; Brahim, S.; Ishihara, K.; Guiseppi-Elie, A. *Biomaterials* **2005**, *26*, 4767−4778.
(18) van de Wetering, P.; Moret, E. E.; Shuurmans-Nieuwenbroek, N. M. E.; van Steenbergen, M. J.; Hennink, W. E. *Bioconjugate Chem.* **1999**, *10*, 589−597.
(19) Even, M.; Haddleton, D. M.; Kukulj, D. *Eur. Polym. J.* **2003**, *39*, 633−639.
(20) Triftaridou, A. I.; Hadjiyannakou, S. C.; Vamvakaki, M.; Patrickios, C. S. *Macromolecules* **2002**, *35*, 2506−2513.
(21) Brahim, S.; Narinesingh, D.; Guiseppi-Elie, A. *Biomacromolecules* **2003**, *4*, 497−503.
(22) Brahim, S.; Narinesingh, D.; Guiseppi-Elie, A. *Biomacromolecules* **2003**, *4*, 1224−1231.
(23) Mathew-Krotz, J.; Mahadevan, V. *Macromol. Chem. Phys.* **1997**, *198*, 1597−1604.
(24) Snijder, A.; Klumperman, B.; vand der Linde, R. *Macromolecules* **2002**, *35*, 4785−4790.
(25) Young, R. J.; Lovell, P. A. *Introduction to Polymers*, 2nd ed.; Chapman & Hall: London, 1991.
(26) Coppola, G.; Fabbri, P.; Pallesi, B.; Bianchi, U. *J. Appl. Polym. Sci.* **1972**, *16*, 2829-2834.
(27) *Polymer Handbook*, 4th ed.; Brandrup, J., Immergut, E. H., Grulke, E. A., Eds.; Wiley-Interscience: New York, 1999.
(28) Matyjaszewski, K.; Shipp, D. A.; Wang, J.-L.; Grimaud, T.; Patten, T. E. *Macromolecules* **1998**, *31*, 6836−6840.
(29) Shellekens, M. A.; de Wit, F.; Klumperman, B. *Macromolecules* **2001**, *34*, 7961−7966.
(30) Wang, T.-L.; Liu, Y.-Z.; Jeng, B.-C.; Cai, Y.-C. *J. Polym. Res.* **2005**, *12*, 67−75.
(31) Matyjaszewski, K.; Xia, J. *Chem. Rev.* **2001**, *101*, 2921−2990.
(32) Matyjaszewski, K.; Patten, T.; Xia, J. *J. Am. Chem. Soc.* **1997**, *119*, 674−680.
(33) Fischer, H. *J. Polym. Sci., Part A: Polym. Chem.* **1999**, *37*, 1885−1901.
(34) Zhang, H.; Klumperman, B.; Ming, W.; Fischer, H.; van der Linde, R. *Macromolecules* **2001**, *34*, 6169−6173.
(35) Guice, K. B.; Loo, Y.-L. APS Abstract, March 2006 Meeting.
(36) Miller, P. J.; Matyjaszewski, K. *Macromolecules* **1999**, *32*, 8760−8767.
(37) Remp, P.; Merrill, E. W. *Polymer Synthesis*, 2nd ed.; Hüthig & Wepf: Verlag, 1991.
(38) Dias, M. L.; Mano, E. B.; Azuma, C. *Eur. Polym. J.* **1997**, *33*, 559−564.
(39) Dubin, P. L.; Koontz, S.; Wright, K. L. *J. Polym. Sci., Polym. Chem. Ed.* **1977**, *15*, 2047−2057.
(40) *CRC Handbook of Chemistry and Physics*, 86th ed.; Lide, D. R., Ed.; Taylor & Francis: London, 2005.
(41) ASTM D153-84, Standard Test Methods for Specific Gravity of Pigments, 2003.
(42) Porod, G. In *Small-Angle X-ray Scattering*; Glatter, O., Kratky, O., Eds.; Academic Press: London, 1982.
(43) Sakurai, S.; Momii, T.; Taie, K.; Shibayama, M.; Nomura, S.; Hashimoto, T. *Macromolecules* **1993**, *26*, 485−491.
(44) Çaykara, T.; Özyürek, C.; Kanto''lu, Ö.; Güven, O. *J. Polym. Sci., Part B: Polym. Phys.* **2002**, *40*, 1995−2003.
(45) Senshu, K.; Yamashita, S.; Ito, M.; Hirao, A.; Nakahama, S. *Langmuir* **1995**, *11*, 2293−2300.
(46) Matsen, M. W.; Bates, F. S. *Macromolecules* **1996**, *29*, 1091−1098.
(47) Lee, J.; Aoai, T.; Kondo, S.; Myagawa, N.; Takahara, S.; Yamaoka, T. *J. Polym. Sci., Part A: Polym. Chem.* **2002**, *40*, 1858−1867.
(48) Bories-Azeau, X.; Armes, S. P. *Macromolecules* **2002**, *35*, 10241−10243.

MA052667H